Markov flow policy – deep MC

Nitsan Soffair
Nitsan.Soffair@GMAIL.com
Software Information Systems Engineering
Ben Gurion University of the Negev

Gilad Katz
Katz.Gilad@GMAIL.com
Software Information Systems Engineering
Ben Gurion University of the Negev

Abstract

Discounted algorithms often encounter evaluation errors due to their reliance on short-term estimations, which can impede their efficacy in addressing simple, short-term tasks and impose undesired temporal discounts (γ). Interestingly, these algorithms are often tested without applying a discount, a phenomenon we refer as the *train-test bias*. In response to these challenges, we propose the Markov Flow Policy, which utilizes a non-negative neural network flow to enable comprehensive forward-view predictions. Through integration into the TD7 codebase and evaluation using the MuJoCo benchmark, we observe significant performance improvements, positioning MFP as a straightforward, practical, and easily implementable solution within the domain of average rewards algorithms.

1 Introduction

1.1 Reinforcement learning

Reinforcement Learning Sutton & Barto (2018) involves an agent that learns an optimal policy, denoted as $\pi : \mathcal{S} \to \mathcal{A}$, mapping states to actions through trial and error within an environment E. This environment is modeled as a Markov Decision Process (MDP) Bellman (1957), characterized by a state space $\mathcal{S} \in \mathbb{R}^{\dim(\mathcal{S})}$, an action space $\mathcal{A} \in \mathbb{R}^{\dim(\mathcal{A})}$, a reward mechanism $\mathcal{R} \in \mathbb{R}$, and a discount factor $\gamma \in (0, 1]$ representing temporal engineering considerations.

1.2 Future rewards

Q-values estimations Sutton & Barto (2018) based on predictions of future estimations discounted using a small $\gamma < 1$. However, this approach is susceptible to evaluation errors Fujimoto et al. (2018). These errors stem from the assumption made in finite-term predictions that future rewards are negligible (when t becomes very large, Q_t approaches approximately zero), a notion reinforced by the small γ value ($\gamma < 1$). Consequently, the algorithm's predictive capability is constrained beyond a certain timestep, where discounted Q-values become insignificant. For example, many RL algorithms employ a γ value of .99, resulting in a 300-step horizon where $.99^{300} \approx 0.05$.

Definition 1.1. *The train-test bias is a phenomenon in reinforcement learning where an RL algorithm estimates Q-values during training with discounting, but evaluates an agent's performance during testing without discounting.*

It's noteworthy that non-discounted performance metrics are predominantly utilized in the evaluation of trained policies across various reinforcement learning benchmarks, including Atari games Mnih et al. (2013) and MuJoCo Todorov et al. (2012).

1.3 Temporal paradigms

Reinforcement learning is typically classified into two primary temporal paradigms:

Preprint. Under review.

1. **Discounted rewards**: This paradigm demonstrates satisfactory performance but grapples with evaluation errors, particularly concerning short-horizon-based future predictions.
2. **Average rewards** Mahadevan (1996): Despite offering less satisfactory performance, this paradigm presents an intriguing real-life challenge: learning predictions based on a full infinite-horizon perspective.

Algorithms that rely on average rewards encounter difficulties because they require infinite predictions of Q-values. To tackle this challenge, R-learning Schwartz (1993) incorporates the concept of average values by integrating ρ_ϕ (as defined in Equation 1) into the estimation of the Q-function. The average values mechanism immediately averages all future rewards to the agent without incorporating any form of discounting, akin to providing a constant per-timestep reward similar to a fixed salary.

As n tends towards infinity ($n \to \infty$), the sensitivity of ρ to a state s increases. ρ^π represents a per-trajectory value, indicating that $\rho^\pi(s)$ is approximately equal to $\rho^\pi(s')$ if s and s' belong to the same trajectory τ under policy π. This property facilitates the swift propagation of R-values through updates.

$$\underbrace{\rho^\pi(s)}_{\textit{deep MC. Metropolis \& Ulam (1949)}.} = \lim_{n\to\infty} \frac{\overbrace{V^\pi_{(n)}(s)}^{\text{Total rewards} - \sum_{t=0}^{n-1}\mathbb{E}[r^\pi_{s,t}]}}{\underbrace{n}_{\text{Total steps.}}} \tag{1}$$

The discount factor, stemming from economic principles such as operations research Schwartz (1993), serves as a representation of the interest rate. Nevertheless, it also introduces a practical constraint similar to the concept of a finite lifetime for the agent. Fundamentally, the discount factor serves a core practical purpose: approximating an infinite sum of rewards into a finite real number.

Blackwell optimality Blackwell (1962) entails the lexicographical maximization of an infinite series, with ρ and σ (2) (Schwartz, 1993, page 3) denoting the first two terms of this series.

$$\underbrace{\sigma^\pi(s)}_{\text{Infinite-step average error.}} = \lim_{n\to\infty} \frac{\sum_{m=0}^{n-1}[\underbrace{V^\pi_{(m)}(s) - m\cdot\rho^\pi(s)}_{m\text{-step error.}}]}{n} \tag{2}$$

The connection between discounted to undiscounted estimations can be summarized by (3) (Schwartz, 1993, page 4):

$$V^\pi_\gamma(s) = \underbrace{\frac{\rho^\pi(s)}{1-\gamma}}_{\approx\infty \text{ (when } \gamma\to 1)} + \underbrace{\sigma^\pi(s)}_{\text{Average values error.}} + \underbrace{\epsilon(s,\gamma)}_{\text{Discount error.}}, \quad \lim_{\gamma\to 1}\epsilon(s,\gamma) = 0 \tag{3}$$

Thus on the undiscounted case ($\gamma = 1$) we get (4):

$$V^\pi_\gamma(s) \approx \frac{\rho^\pi(s)}{1-\gamma} \propto \underbrace{\rho^\pi(s)}_{\text{State value.}} \tag{4}$$

Which is basically a practical deep estimation to first visit MC (4) Metropolis & Ulam (1949) which does not use a discount for evaluations.

1.4 Generative flow networks

Generative flow networks, detailed in Bengio et al. (2021), are neural network structures primarily geared towards generative tasks, notable for their ability to retain complete memory via energy flow.

In our research, we introduce Markov Flow Policy, a novel algorithm crafted to address the evaluation error prevalent in discounted RL setups, particularly in tasks with elongated horizons. MFP stands as

a straightforward remedy, seamlessly integrating into RL frameworks and offering a solution to the challenges posed by the average rewards temporal paradigm. Our findings showcase its efficacy, akin to a much-needed panacea, in tackling these issues.

2 Markov flow policy

Flow networks Bengio et al. (2021), exhibit distinctive characteristics that differentiate them from traditional neural networks. These networks adhere to the principle of fixed energy, maintaining a consistent energy level that does not fluctuate over time and aligned with non-discounted reinforcement learning paradigm Mahadevan (1996).

Markov flow policy is an reinforcement learning algorithm rooted in energy principles, ensuring zero energy loss. MFP leverages a Markovian flow-based neural network architecture, relying on the fundamental property of non-negative data flow.

Integration of MFP into existing RL frameworks requires minimal coding effort. In the context of deep policy-based RL setups, enforcing non-negative flow involves simply applying the absolute function to the policy's flow (2), ensuring that data flows non-negatively from the source to the target layer.

By setting γ to 1, a practical implementation of deep first-visit Monte Carlo (4) Metropolis & Ulam (1949) emerges, firmly grounded in the principles of generative flow networks.

The core essence of MFP can be encapsulated in its policy code, which includes the application of the absolute function to the flow (**a.abs()**, (2)).

```
        def forward(self, state, zs):
            a = AvgL1Norm(self.l0(state))
            a = torch.cat([a, zs], 1)

            a = self.activ(self.l1(
                a.abs()
            ))
            a = self.activ(self.l2(
                a.abs()
            ))

            return torch.tanh(self.l3(a))
```

3 Experiments

The implementation of the Markov Flow Policy is constructed atop TD7's codebase ([1]), offering a transparent integration of prominent continuous optimistic-pessimistic deep RL algorithms like DDPG (optimistic), TD3 (pessimistic), and TD7 (pessimistic) Lillicrap et al. (2015); Fujimoto et al. (2018, 2023).

To assess the performance of MFP, we conduct evaluations using the MuJoCo-suite Todorov et al. (2012), varying the timestep ranges from 1 million to 10 million and across 10 distinct seeds (indexed from 0 to 9). This comprehensive evaluation encompasses a wide range of action-space sizes, spanning from Hopper (3) to Humanoid (17), and covers the full spectrum of optimistic-pessimistic properties, incorporating both DDPG and TD3 algorithms. Additionally, we explore the full range of computational power, from 1 million to 10 million timesteps.

Our results are presented through dynamic interactive plots, illustrating average rewards and standard errors at each timestep (refer to 3.2.1), supplemented by a concise table showcasing maximum average rewards percentage improvements and average percentage improvements (refer to 3.2.2, 3.2.2).

[1] `https://github.com/anonymouszxcv16/MFP`.

3.1 Environments

We evaluate the performance of MFP using various MuJoCo-based environments Todorov et al. (2012), including:

1. **HalfCheetah** ($\dim(\mathcal{A}) = 6$, $\underbrace{\mathcal{T}}_{\text{Horizon}} = 1,000$): This environment focuses on two-legged locomotion, challenging the agent to propel a cheetah forward as swiftly as possible.
2. **Ant** ($\dim(\mathcal{A}) = 8$, $\underbrace{\mathcal{T}}_{\text{Horizon}} = 1,000$): In this scenario, the task involves four-legged locomotion, with the primary objective being for an ant to move forward while maintaining balance.
3. **Humanoid** ($\dim(\mathcal{A}) = 17$, $\underbrace{\mathcal{T}}_{\text{Horizon}} = 1,000$): This environment simulates locomotion, requiring a humanoid figure equipped with two legs and two arms to walk forward steadily without losing balance.

3.2 Results

The outcomes were computed using hardware featuring an NVIDIA GPU GeForce RTX 3050 and an Intel Core i9-12900KF processor with 24 cores and 64-bit architecture, coupled with 16.0 GB of RAM.

3.2.1 Plots (3.2.1)

Average rewards and standard deviations (Optimistic setting, 1 million timesteps, discount factor $\gamma = 0.99$, exploration noise $\mathcal{N} = .1$ (Lillicrap et al., 2015, page 4), hardware 3.2) (3.2.1).

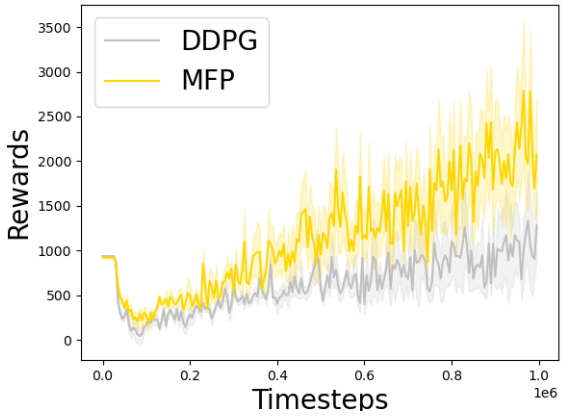

Figure 1: Ant ($\dim(\mathcal{A}) = 8$).

MFP consistently outperforms DDPG across multiple seeds on the ant environment, demonstrating superior performance throughout the entire learning phase, especially notable in its more favorable learning curve.

3.2.2 Tables (3.2.2, 3.2.2)

Maximum achieved average rewards and percentage enhancement (Optimistic condition, 1 million timesteps, discount factor $\gamma = 0.99$, exploration noise $\mathcal{N} = .1$ (Lillicrap et al., 2015, page 4), hardware 3.2) (3.2.2).

Environment	DDPG	MFP	Improvement
HalfCheetah	**11,711.8**	7,051.5	-39.8%
Ant	1,332.9	**2,789.4**	**+109.3**%
Humanoid	**675.9**	533.8	-21.0%
Average			**+16.16**%

Table 1: HalfCheetah ($\dim(\mathcal{A}) = 6$), Ant ($\dim(\mathcal{A}) = 8$) and Humanoid ($\dim(\mathcal{A}) = 17$).

MFP exhibits a noticeable performance superiority over DDPG across ten different seeds and one million timesteps across the half-cheetah, ant, and humanoid environments, showcasing an average improvement of **+16.16**%.

The peak average rewards achieved and the corresponding percentage enhancement (in an optimistic setting, with 10 million timesteps and 2 seeds, utilizing a discount factor of $\gamma = 0.99$, exploration noise $\mathcal{N} = .1$ (Lillicrap et al., 2015, page 4), hardware 3.2) (3.2.2).

Environment	DDPG	MFP	Improvement
Humanoid-v2	4,656.8	**6,442.2**	**+38.3**%
Average			**+38.3**%

Table 2: Humanoid ($\dim(\mathcal{A}) = 17$).

4 Related work

Generative flow networks Bengio et al. (2021) aim to maintain positive energy flow from source to destination, ensuring zero energy loss. GFlowNets adhere to flow-consistency equations akin to non-discount-based R-values, ensuring a consistent energy flow. The objective is to establish fixed flow-based evaluations where energy moves immediately. Trajectory balance (TB) Malkin et al. (2022) minimizes flow-matching and detailed balance objectives, aiming to balance forward and backward flow consistency.

Q-learning Watkins & Dayan (1992) is a tabular off-policy RL algorithm with advantages including optimality and avoiding infinite cycles. In contrast, R-learning (*Average Q-learning*) Schwartz (1993) (4) is a tabular off-policy model-free algorithm without a discount factor, converging faster and being more explorative.

Algorithm 1 R-learning

1: **for** each iteration **do**
2: Take an action a at state s – observe immediate reward r_{imm} and state next s'.
3: Update R by:

$$R(s,a) \overset{\beta}{\leftarrow} \underbrace{r_{\text{imm}} + \underbrace{\underbrace{U_R(s')}_{\max_{a'} R(s',a')} - \underbrace{\rho}_{\text{Average values.}}}_{\text{Average } Q-\text{target.}}}_{} \tag{5}$$

4: **if** $a = \underbrace{\arg\max_a U_R(s)}_{\text{Best action selected.}}$ **then**
5: $\rho \overset{\alpha}{\leftarrow} \underbrace{r_{\text{imm}} + U_R(s') - U_R(s)}_{\text{TD-error.}}$
6: **end if**
7: **end for**

H-learning Tadepalli & Ok (1998), positioned between R-learning and Adaptive RTDP Barto et al. (1995), exhibits robustness to exploration policies. The pseudocode for H-learning captures its essence as a robust off-policy algorithm.

The Monte Carlo method Metropolis & Ulam (1949) originated in the realm of mathematical physics and was later extended to a fundamental class of reinforcement learning algorithms. At its core, this method revolves around a basic concept: as more returns R_t are observed, the average returns ρ should converge to the expected value V (Sutton & Barto, 2018, page 92).

Consider the scenario where we aim to estimate $v_\pi(s)$, the value of a state s under policy π, based on a set of episodes obtained by following π and traversing through s. Each instance of encountering state s in an episode is termed a visit to s. Naturally, s might be visited multiple times within the same episode; the initial visit to s in an episode is designated as the first visit to s. The first-visit Monte Carlo method estimates $v_\pi(s)$ by averaging the returns following the first visits to s.

First-visit Monte Carlo prediction for approximating $V \approx v_\pi$ can be expressed by 4 (Sutton & Barto, 2018, page 92).

Algorithm 2 First-visit MC

for each episode **do**
  Generate an episode following $\pi : S_0, A_0, R_1, S_1, \ldots, S_{T-1}, A_{T-1}, R_T$.
  $G \leftarrow 0$
  for each step $t = T-1, T-2, \ldots, 0$ **do**
    $G \leftarrow \gamma G + R_{t+1}$
    if $S_t \notin \{S_0, S_1, \ldots, S_{t-1}\}$ **then**
      Append G to Returns(S_t)
      $V(S_t) \leftarrow$ average(Returns(S_t))
    end if
  end for
end for

5 Discussion and Conclusion

The Markov Flow Policy presents a straightforward average rewards algorithm, addressing a broad range of RL challenges, notably the *train-test-bias* (1.1), where evaluations of Q are mismatched between training and testing paradigms (Bengio et al., 2021, page 4). Leveraging the core property of generative flow networks, MFP incorporates a Markov flow property, ensuring non-negative flow within the neural network policy (Bengio et al., 2021, page 4), minimizing data loss through flow-based energy.

Implemented atop the TD7 codebase Fujimoto et al. (2023), MFP is evaluated across a spectrum of computational resources from 1 to 10 million timesteps, exploring diverse environments ranging from 6 to 17 dimensions in action space Todorov et al. (2012), and spanning various RL algorithm types from optimistic (DDPG Lillicrap et al. (2015)) to pessimistic (TD3 Fujimoto et al. (2018)). Results demonstrate MFP's significant performance advantage, particularly in scenarios benefiting from its exploratory properties.

However, MFP exhibits limitations, particularly evident in complex exploration tasks with high-dimensional action spaces, such as humanoid with 17 dimensions. In such cases, MFP necessitates substantial computational resources, exemplified by the requirement for 10 million timesteps to achieve satisfactory performance.

References

Andrew G Barto, Steven J Bradtke, and Satinder P Singh. Learning to act using real-time dynamic programming. *Artificial intelligence*, 72(1-2):81–138, 1995.

Richard Bellman. A markovian decision process. *Journal of mathematics and mechanics*, pp. 679–684, 1957.

Emmanuel Bengio, Moksh Jain, Maksym Korablyov, Doina Precup, and Yoshua Bengio. Flow network based generative models for non-iterative diverse candidate generation. In M. Ranzato, A. Beygelzimer, Y. Dauphin, P.S. Liang, and J. Wortman Vaughan (eds.), *Advances in Neural Information Processing Systems*, volume 34, pp. 27381–27394. Curran Associates,

Inc., 2021. URL https://proceedings.neurips.cc/paper_files/paper/2021/file/e614f646836aaed9f89ce58e837e2310-Paper.pdf.

David Blackwell. Discrete dynamic programming. *The Annals of Mathematical Statistics*, pp. 719–726, 1962.

Scott Fujimoto, Herke Hoof, and David Meger. Addressing function approximation error in actor-critic methods. In *International conference on machine learning*, pp. 1587–1596. PMLR, 2018.

Scott Fujimoto, Wei-Di Chang, Edward J Smith, Shixiang Shane Gu, Doina Precup, and David Meger. For sale: State-action representation learning for deep reinforcement learning. *arXiv preprint arXiv:2306.02451*, 2023.

Timothy P Lillicrap, Jonathan J Hunt, Alexander Pritzel, Nicolas Heess, Tom Erez, Yuval Tassa, David Silver, and Daan Wierstra. Continuous control with deep reinforcement learning. *arXiv preprint arXiv:1509.02971*, 2015.

Sridhar Mahadevan. Average reward reinforcement learning: Foundations, algorithms, and empirical results. *Machine learning*, 22(1):159–195, 1996.

Nikolay Malkin, Moksh Jain, Emmanuel Bengio, Chen Sun, and Yoshua Bengio. Trajectory balance: Improved credit assignment in gflownets. *Advances in Neural Information Processing Systems*, 35: 5955–5967, 2022.

Nicholas Metropolis and Stanislaw Ulam. The monte carlo method. *Journal of the American statistical association*, 44(247):335–341, 1949.

Volodymyr Mnih, Koray Kavukcuoglu, David Silver, Alex Graves, Ioannis Antonoglou, Daan Wierstra, and Martin Riedmiller. Playing atari with deep reinforcement learning. *arXiv preprint arXiv:1312.5602*, 2013.

Anton Schwartz. A reinforcement learning method for maximizing undiscounted rewards. In *Proceedings of the tenth international conference on machine learning*, volume 298, pp. 298–305, 1993.

Richard S Sutton and Andrew G Barto. *Reinforcement learning: An introduction*. MIT press, 2018.

Prasad Tadepalli and DoKyeong Ok. Model-based average reward reinforcement learning. *Artificial intelligence*, 100(1-2):177–224, 1998.

Emanuel Todorov, Tom Erez, and Yuval Tassa. Mujoco: A physics engine for model-based control. In *2012 IEEE/RSJ international conference on intelligent robots and systems*, pp. 5026–5033. IEEE, 2012.

Christopher JCH Watkins and Peter Dayan. Q-learning. *Machine learning*, 8:279–292, 1992.